Rotationally Resolved Infrared Spectroscopy of the Hydroxymethyl Radical (CH$_2$OH)[†]

Lin Feng, Jie Wei, and Hanna Reisler*

Department of Chemistry, University of Southern California, Los Angeles, California 90089-0482

Received: February 5, 2004

Infrared spectra of CH$_2$OH have been recorded in the molecular beam using a combination of depletion and double resonant ionization detected IR (DRID-IR) spectroscopy via the 3p$_z$ Rydberg state. With DRID-IR spectroscopy, IR transitions are detected by exciting CH$_2$OH in a selected vibrational level in the ground state to a Franck–Condon favorable level in 3p$_z$ from which it is ionized. Rotationally resolved spectra of the fundamental CH symmetric stretch (ν_3), CH asymmetric stretch (ν_2), OH stretch (ν_1), and the first OH-stretch overtone ($2\nu_1$) are obtained. The rovibrational structure is analyzed with the aid of ab initio calculations and asymmetric rotor simulations. The OH and CH symmetric stretch fundamentals are hybrid *a/b*-type bands. On the other hand, a pure *b*-type transition is observed for the CH asymmetric stretch fundamental. The spectrum of the first overtone of the OH stretch is rotationally resolved, indicating that intramolecular vibrational redistribution (IVR) is not extensive. The rotational linewidth, however, is ~0.8 cm^{-1}, greater than the laser-limited linewidth observed for the fundamental transitions (~0.4 cm^{-1}). Reasons for the increase in linewidth are discussed.

I. Introduction

The hydroxymethyl radical (CH$_2$OH) and its isomer, the methoxy radical (CH$_3$O), are important intermediates in hydrocarbon combustion and atmospheric processes.[1–6] Insights into intramolecular vibrational redistribution (IVR), isomerization, and unimolecular dissociation on the ground potential energy surface (PES) of CH$_2$OH can be obtained from spectroscopic investigations of its fundamental and overtone vibrational transitions. According to ab initio calculations, CH$_2$OH requires ~16000 cm^{-1} to surmount the barrier to H + CH$_2$O(^{1}A$_1$) on the ground state,[7,8] while the barrier to CH$_3$O decomposition has been determined experimentally to be only ~ 11000 cm^{-1} relative to the energy of CH$_2$OH.[9–11] The height of the isomerization barrier (calculated at ~14000 cm^{-1})[8,12,13] will therefore dictate whether the CH$_2$OH radical can decompose via the isomerization route. It is expected that the low barriers to isomerization and dissociation would result in increased anharmonicity, thereby promoting IVR and isomerization to CH$_3$O.

The equilibrium structure of CH$_2$OH on the ground state, if treated as a rigid body, belongs to the C_1 point group.[14] The pyramidal geometry reduces the occupation of the π^*_{CO} singly occupied antibonding orbital and lowers the total energy of the radical. Johnson and Hudgens found that in excitation to 3p Rydberg states, vibronic transitions involving the OH torsion (ν_8) and CH$_2$ wag (ν_9) modes obeyed a "Δv = even" selection rule.[14] The derived frequencies of ν_8 and ν_9 agreed well with results obtained by ab initio calculations. They explained this behavior by considering the finite barriers of OH torsion (1643 cm^{-1}) and CH$_2$ wag (156 cm^{-1}) and concluded that the radical's electronic wave function complied with the C_s point group. Two recent theoretical investigations by Marenich et al. confirm the low barrier (140 cm^{-1}) along the CH$_2$ inversion pathway.[15,16] As a result, the two mirror-image equilibrium structures of C_1

symmetry rapidly interconvert; therefore, CH$_2$OH in its ground state can be treated as a planar molecule of C_s symmetry. In addition, the calculated heat of formation reported by Johnson et al.[14] and Marenich et al.[15,16] agrees well with the measured enthalpies of formation of CH$_2$OH when the zero-point energy is calculated by taking into account structural flexibility and anharmonicity. On the basis of these considerations, the ground state of CH$_2$OH has been labeled 1^{2}A$''$.

Studies of excited Rydberg states of CH$_2$OH have shown that following internal conversion, the radical dissociates on the ground PES. Electronic spectra of the hydroxymethyl radical involving transitions to the 3s, 3p$_x$, and 3p$_z$ Rydberg states have been measured by ultraviolet (UV) absorption,[3] resonance-enhanced multiphoton ionization (REMPI),[14,17–20] and depletion spectroscopy.[21] All of the transitions are lifetime-broadened by predissociation. The vibronic bands of the 2^{2}A$''$(3p$_z$) ← 1^{2}A$''$ transition are the narrowest, having 11 cm^{-1} homogeneous linewidth.[17] The final dissociation step of these Rydberg states proceeds on the ground-state PES reached through 3s/ground-state conical intersections.[22,23] Even though ground-state CH$_2$OH with high internal energy is generated, no evidence of CH$_2$OH ↔ CH$_3$O isomerization has been obtained. Conical intersection calculations by Hoffman and Yarkony suggest that the intersection seam between the 3s and ground states is located in the repulsive region in the O–H coordinate, disfavoring isomerization.[22]

Knowledge of the vibrational spectroscopy of the radical is prerequisite to understanding the competition between CH$_2$OH ↔ CH$_3$O isomerization and direct O–H bond fission on the ground PES. Early experiments on CH$_2$OH infrared (IR) spectroscopy were carried out in argon and nitrogen matrixes,[24,25] and vibrational bands involving the OH (ν_1) and CO (ν_6) stretches, CH$_2$ scissors (ν_4), in- (ν_5) and out-of-phase (ν_7) HCOH bends, and torsion (ν_8) were observed. In flow reactor (300 K) studies of REMPI spectroscopy via the 3p$_z$ state,[14] transitions from vibrational "hot bands" of CH$_2$OH on the ground state were identified, and ν_6, ν_8, and the CH$_2$ wag (ν_9) frequencies
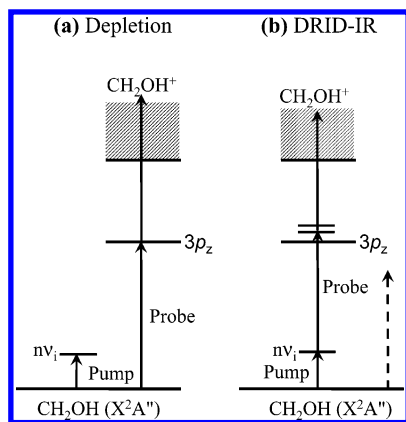

Figure 1. Schematic diagrams of (a) depletion and (b) DRID-IR spectroscopy methods.

were determined. The two CH stretch vibrations, ν_2 and ν_3, were not observed and no rotationally resolved spectra were reported.

Molecular-beam spectroscopy reduces spectral congestion and enables studies of rotationally resolved spectra of fundamentals and low-energy overtones. Despite its small size, the vibrational spectroscopy of CH_2OH can be rather complex. Both OH- and CH-stretches serve as chromophores for vibrational excitation and irregular vibrational energy patterns have been calculated for the coupled ν_8 and ν_9 modes.[14] Spectral patterns observed in high-overtone excitation can shed light on IVR, isomerization, and unimolecular dissociation mechanisms.

In this paper, we report the first observations of rotationally resolved OH- and CH-stretch vibrational transitions in CH_2OH, obtained in a molecular beam by using double resonance ionization detected IR (DRID-IR) spectroscopy. A similar scheme has been exploited before in studying IR absorption of molecules.[26-29] In this method, a supersonically cooled radical is excited to a vibrational level of the electronic ground state by IR laser radiation. The vibrationally excited radical is selectively ionized by a resonant two-photon process via a Franck−Condon favorable transition to an upper electronic state (e.g., the $3p_z$ Rydberg state for CH_2OH). This technique, which is based on ionization detection, is sensitive and largely background free. Furthermore, the observed spectra are species-selective, since only cations of a specific mass are detected. This is especially important in studies of radicals produced by chemical reactions and in electrical discharges.

II. Experiment

The experimental arrangement and radical generation method have been described in detail elsewhere.[17,30] A mixture of 4% CH_3OH (Aldrich, used without further purification) and ∼1% Cl_2 (Airgas, Inc., 99.5%) in He at 2 atm total pressure is prepared in a 4-L glass bulb. A piezoelectrically driven pulsed nozzle operating at 10 Hz introduces this mixture to the source region of a differentially pumped vacuum chamber. A 355-nm pulsed laser beam (Spectra Physics, GCR-11; 8 mJ, focused by a 30 cm f.l. cylindrical lens) crosses the edge of a 1-mm diameter quartz tube attached in front of the nozzle orifice. The 355-nm radiation dissociates Cl_2, and the Cl atoms react rapidly with CH_3OH, producing CH_2OH. The radicals generated in the collisional part undergo cooling during the supersonic expansion and pass through a 1.51-mm diameter skimmer (Beam Dynamics) before reaching the detection region.

A. Depletion and Double Resonant Ionization Detected IR (DRID-IR) Spectroscopy. Figure 1 shows excitation schemes for depletion and DRID-IR spectroscopy. Tunable IR

radiation from a seeded Nd:YAG laser pumped optical parameter oscillator and amplifier (OPO/OPA, LaserVision, 20 cm f.l. lens) is used to excite the radical to a selected vibrational state in the ground state. To avoid absorption of the IR radiation by atmospheric water, N_2 purge tubes are used in the optical path of the IR laser beam to the detection chamber. The photoacoustic spectrum of CH_4 in the range 2900−3200 cm^{-1} serves to calibrate the IR frequency and to estimate the IR laser bandwidth (0.4 cm^{-1}).[31] With this bandwidth, individual rotational lines of the IR spectrum are resolved.

The UV probe radiation is obtained from another seeded Nd: YAG laser pumped OPO/OPA (Continuum, PL8000/Sunlite/ FX-1; 40 cm f.l. lens). The pump and probe laser beams are counterpropagating and cross the molecular beam at right angle. The time delay between them is ∼20 ns.

In the depletion scheme shown in Figure 1a, the probe laser beam frequency is fixed at 41062 cm^{-1} to access the peak of the CH_2OH $2^2A''(3p_z) \leftarrow 1^2A''$ origin band.[17] The population of the ground state is depleted whenever IR absorption to a vibrationally excited state takes place, thereby attenuating the CH_2OH^+ ion signal obtained by 1+1 REMPI. The depletion method is straightforward and exploits the known Franck−Condon factors (FCFs) for the UV REMPI transition.[32-34] It was used before to assign the electronic transitions to the 3s and $3p_x$ Rydberg states.[21] Therefore, we have used it to pinpoint spectral locations of the vibrational transitions in the ground state. However, the large CH_2OH^+ ion signals generated by the probe laser beam reduce the signal-to-noise (S/N) ratio.

In DRID-IR spectroscopy (Figure 1b), the UV frequency is adjusted to excite CH_2OH in a selected rovibrational state in the ground state to a Franck−Condon favorable vibronic level in the $3p_z$ Rydberg state and then to further ionize it. Rovibrational spectra are recorded by tuning simultaneously the IR and UV laser frequencies and fixing their total energy at the peak of the transition to the selected vibronic level in $3p_z$. This scheme takes advantage of the broad homogeneous linewidth of the rotational lines of the transition to the $3p_z$ state (>10 cm^{-1}).[14,17] The UV beam (probe) frequency is not resonant with any of the vibronic transitions from ground-state CH_2OH, and hence no ion signal is detected in the absence of IR radiation. A 20-ns delay between the IR and UV laser beams ensures that there is no ion signal from nonresonant IR+UV excitation of the vibrational ground state. The major advantage of DRID-IR over depletion spectroscopy is that it is largely background free. The primary prerequisite for its successful application is the existence of a vibronic transition with a good Franck−Condon factor from the vibrationally excited state to the $3p_z$ Rydberg state.

Depletion and DRID-IR spectra are recorded in both "IR on" and "IR off" conditions. In IR on conditions, the probe laser is fired 20 ns after the pump laser, while with IR off, the probe laser precedes the pump laser by 1 μs. The time delay is regulated by digital pulse/delay generators (DG 535, Stanford Research Systems, 10-ns resolution). Each data point is an average of 50 measurements.

B. IR+UV REMPI Spectroscopy. The goal of this experiment is to locate vibronic resonances with large FCFs in the $3p_z$ state for DRID-IR spectroscopy. The IR laser beam frequency is fixed at the position of maximum absorption in the depletion spectra, while the UV frequency is scanned in the energy region around 41 062 cm^{-1}, the peak of the origin band of the $2^2A''(3p_z) \leftarrow 1^2A''$ transition. The IR and UV radiation sources are the same as those used in the depletion and DRID-IR experiments.

Rotationally Resolved Infrared Spectroscopy

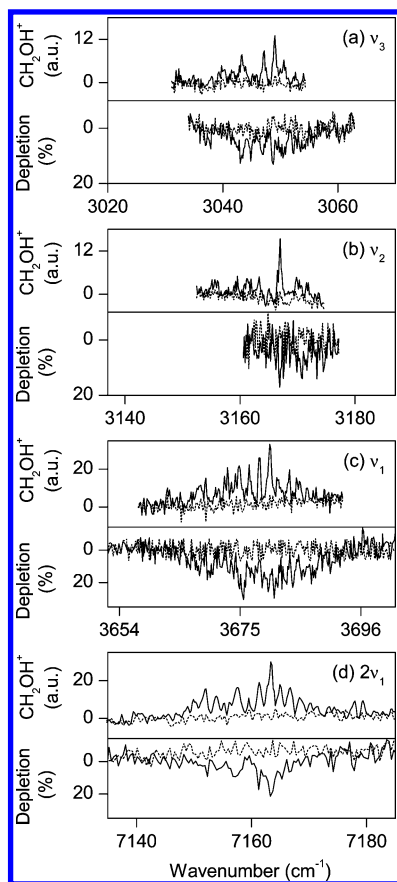*J. Phys. Chem. A, Vol. 108, No. 39, 2004* **7905**

Figure 2. IR spectra of CH_2OH in the region of the fundamentals of (a) CH symmetric stretch (ν_3); (b) CH asymmetric stretch (ν_2); (c) OH stretch (ν_1); and (d) first overtone of OH stretch ($2\nu_1$). In each panel, the upper trace depicts the DRID-IR spectrum and the bottom trace is the depletion spectrum. Solid and dotted lines represent signals corresponding to "IR-on" and "IR-off", respectively. The IR energy is 10 mJ in depletion and 4 mJ in DRID-IR.

III. Results

Figure 2 displays infrared spectra of CH_2OH in the region of the (a) CH symmetric stretch (ν_3), (b) CH asymmetric stretch (ν_2), (c) OH stretch (ν_1), and (d) first OH-stretch overtone ($2\nu_1$). The spectra are recorded using DRID-IR (upper trace) and depletion (bottom trace) spectroscopy, with the solid and dotted lines representing IR on and IR off data, respectively. The intensities in the DRID-IR traces are given as CH_2OH^+ ion signal intensities, which are roughly proportional to the absorption cross section, while the relative absorption in the depletion experiment is calculated as the percent reduction in the CH_2OH^+ ion signal with IR on:

$$I_{\text{absorption}} = \frac{I_{\text{pumpoff}} - I_{\text{pumpon}}}{I_{\text{pumpoff}}} \times 100\%$$

The peak positions in the depletion and DRID-IR spectra are similar, but S/N in the DRID-IR spectra is better.

In depletion experiments, the UV frequency is fixed at the origin band of the $2^2A''(3p_z) \leftarrow 1^2A''$ transition (41 062 cm^{-1}).[14,17] DRID-IR spectra are recorded by pumping the excited vibrational state to a Franck−Condon favorable vibronic level in the $3p_z$ Rydberg state, which is then ionized. The vibronic levels used for DRID-IR are located by IR+UV REMPI spectroscopy, as described in Section II, and are marked by arrows in Figure 3. In this experiment, the IR laser is fixed at a frequency determined from the depletion spectra and the UV
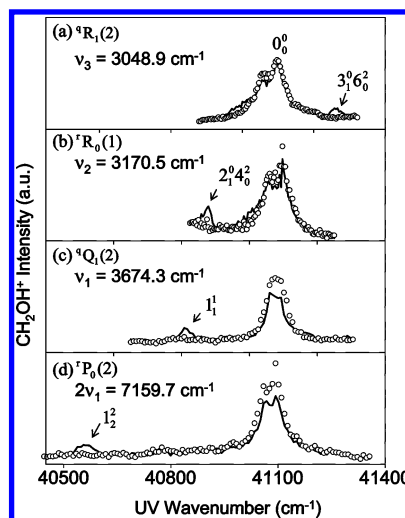

Figure 3. IR+UV REMPI spectrum of CH_2OH obtained via the $3p_z$ state with IR off (open circles), and IR frequency tuned to (solid line) (a) the CH symmetric stretch at 3048.9 cm^{-1} [$^qR_1(2)$]; (b) the CH asymmetric stretch at 3170.5 cm^{-1} [$^rR_0(1)$]; (c) the OH stretch at 3674.3 cm^{-1} [$^qQ_1(2)$]; and (d) its first overtone at 7159.7 cm^{-1} [$^rP_0(2)$]. The IR and UV energies are 4 mJ and 1 mJ, respectively. The arrow in each panel indicates the vibronic transition used in the DRID-IR spectrum shown in the corresponding panel in Figure 2.

laser is scanned around the peak of the $2^2A''(3p_z) \leftarrow 1^2A''$ origin band of CH_2OH. The assignment of the rovibrational level in the ground state, which is listed at the top of each panel, is discussed in Section IV.

The open circles in Figure 3 depict the 1+1 REMPI spectrum of CH_2OH obtained with the IR laser off, while the solid line marks the IR+UV REMPI spectrum. Two features are prominent in the IR on spectra. The first is a decrease in the intensity of the origin band at 41 062 cm^{-1} as a result of depletion of ground-state population by IR absorption. This is most prominent in the ν_1 spectrum and is barely discernible for the ν_2 and ν_3 fundamentals whose oscillator strengths are much lower.

New vibronic bands associated with UV excitation of the IR-excited vibrational state to Franck−Condon favored levels in the $3p_z$ state are also seen in Figure 3. The appearance of these features suggests that the ion signal can be significantly enhanced by choosing specific resonances in $3p_z$, as required by DRID-IR. As discussed elsewhere,[35] this method also allows assignment of new vibronic levels in the $3p_z$ state that are inaccessible by REMPI from the ground vibrational state. The selectivity in the UV excitation, however, points to a limitation of DRID-IR spectroscopy, namely, difficulties in accurate determination of relative intensities of IR transitions. Assuming constant ionization efficiency, the measured CH_2OH^+ signal intensity is a combination of the IR excitation dipole strength and the Franck−Condon factor to the selected vibronic level in $3p_z$.

We searched for vibrational transitions involving combination bands, especially those of the OH stretch with the torsional mode ν_8. The corresponding transitions have been seen in the spectra of methanol and hydroxylamine, albeit with much lower intensities than the OH fundamental.[36,37] We could not identify such transitions above the noise level, indicating that with our detection method, their intensities are at least an order of magnitude lower than the stretch fundamentals.

IV. Discussion

A. Spectral Assignments of Fundamental OH and CH Stretch Transitions. The DRID-IR vibrational spectra shown

TABLE 1: Theoretical and Experimental Constants for the ν_1, ν_2, and ν_3 Fundamentals

	harmonic frequency (cm^{-1})		infrared intensity (km/mol)	$R = I_b/I_a$		rotational constants (cm^{-1})$_{obs}$^{b,c}		
mode	ν_{calc}^{a}	ν_{obs}	I_{calc}	R_{calc}	R_{obs}	A_1	B_1	C_1
ν_3 CH sym str	3013.6	3043.4	18.4	0.1	0.6 ± 0.4	6.48	0.98	0.88
ν_2 CH asym str	3128.2	3161.5	11.2	pure b	pure b	6.41	0.97	0.88
ν_1 OH stretch	3686.7	3674.9	54.9	1.2	0.8 ± 0.4	6.41	0.96	0.88

^{a} The calculated frequencies are scaled by 0.95. ^{b} The calculated zeroth-level rotational constants are $A_0 = 6.51$, $B_0 = 1.00$, $C_0 = 0.88$. ^{c} Error bars: <2%.

in Figure 2 exhibit well-resolved rotational bands. The fundamental OH stretch (ν_1) and CH symmetric stretch (ν_3) transitions have similar rotational structures, while the CH asymmetric stretch (ν_2) is different. To assign the spectra, rotational constants and orientations of the vibrational transition dipole moments were determined by ab initio calculations, and rotational spectra were modeled as asymmetric rotors.

a. Ab Initio Calculations. Ab intio electronic structure calculations of the ground state of CH_2OH were carried out with the ACES II program package[38] and gave the radical's (a) equilibrium geometry and fundamental vibrational frequencies, (b) IR intensities, and (c) IR transition dipole moment vectors. A calculation based on coupled cluster theory with single and double excitations and perturbative triples corrections [CCSD(T)] was performed.[39] The cc-PVTZ basis set was used in the calculation.[40]

The calculated harmonic frequencies of CH_2OH on the ground state gave good agreement with our experimentally obtained values when scaled by 0.95. Similar scaling factor is reported by Crawford et al. in the calculation of p-benzyne.[41] Table 1 lists the calculated and experimental vibrational frequencies of ν_1, ν_2, and ν_3. It is reasonable to treat these modes as harmonic and apply a scaling factor to the calculated frequencies since the low-frequency out-of-plane modes, OH torsion and CH_2 wag, couple weakly to them. The zeroth-level rotational constants derived from the geometry parameters obtained in the calculations are $A_0 = 6.51$ cm^{-1}, $B_0 = 1.00$ cm^{-1}, and $C_0 = 0.88$ cm^{-1}. The asymmetry parameter κ is calculated to be -0.95, indicating that the ground-state radical is a near-prolate asymmetric top. The vibrational frequencies reported here agree within 50 cm^{-1} with those calculated before, and the zeroth-level rotational constants are similar as well.[14–16,42,43]

Infrared intensities and orientations of the vibrational transition dipole moments were computed for displacements from equilibrium along each normal coordinate. The results show that the transition dipole moments of ν_1, ν_2, and ν_3 lie in the a/b-plane. The ν_1 and ν_3 fundamental transitions are hybrid bands of a/b-type, while the spectrum of ν_2 is a pure b-type transition. The calculated infrared intensity of the ν_1 fundamental is significantly larger than that of ν_2 and ν_3. The calculated infrared intensities and the I_b/I_a ratios are summarized in Table 1. As discussed above, the experimental intensities obtained by DRID-IR spectroscopy are not directly proportional to IR absorption cross sections, but the much weaker depletion of ground-state population observed following ν_2 and ν_3 excitations compared to ν_1 (Figures 2 and 3) is in agreement with the calculated relative intensities.

b. Spectral Modeling. Aided by the ab initio calculations, the rotational structures of the OH stretch and CH asymmetric and symmetric stretch fundamentals have been modeled by using the asymmetric rotor program ASYTOP.[44] In the modeling, high-order parameters of the rotational Hamiltonian (e.g.,
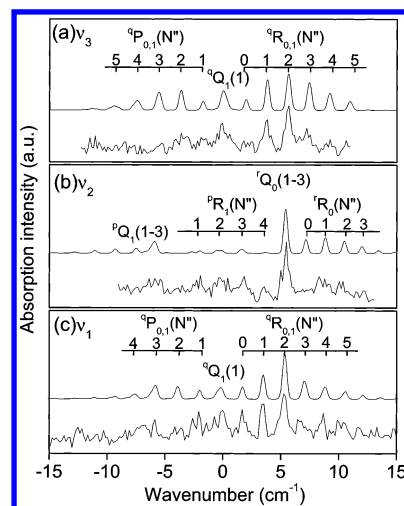

Figure 4. Comparison of experimental spectra of (a) ν_3, (b) ν_2, and (c) ν_1 obtained by DRID-IR spectroscopy with spectral fits. In each panel, the upper spectrum displays the best fit and the bottom spectrum shows experimental data. The spectra in a–c are shifted by 3043.4, 3161.5, and 3674.9 cm^{-1}, respectively. The spectral notations correspond to prolate top rovibrational transitions.

centrifugal distortion, spin-rotation, etc.) are set to zero, and rotational lines are convoluted with a Gaussian width of 0.4 cm^{-1}, corresponding to the IR laser bandwidth. To obtain the values of the band origin and the upper state rotational constants, a least-squares fit is carried out first, in which a rotational temperature $T = 10$ K, estimated from the $1+1'$ two-color REMPI spectrum obtained via the $3p_z$ state, is used.[17] The rotational constants for the lower state and the I_b/I_a ratio are fixed at the calculated values. The values derived from the least-squares fit, with a standard deviation of less than 2%, are listed in Table 1. The rotational constants of the upper state are rather similar to those of the ground vibrational state. In the next step, we vary the I_b/I_a ratio and the rotational temperature to achieve best fits to the measured spectra.

Comparisons of the best fits (upper spectrum) with the DRID-IR spectra (bottom spectrum) are shown in Figure 4. Acceptable fits within our S/N are obtained by using $T = 10 \pm 3$ K and the range of I_b/I_a ratios listed in Table 1. The fitted I_b/I_a ratios are in good agreement with the calculated values. Considering the asymmetry parameter κ value of -0.95, the spectra are also given the traditional $^{\Delta Ka}\Delta N_{Ka''}(N'')$ labels of a prolate symmetric top, as shown in Figure 4.

In summary, the measured vibrational frequencies and types of transitions of the OH and CH fundamentals are in excellent agreement with ab initio calculations. The two CH transitions are different in frequency and transition type, corresponding to CH bonds of different equilibrium bond length.[14] These differences indicate that the radical's electronic structure influences its vibrational spectroscopy. Electronic effects that depend on the relative orientation of molecular orbitals split the frequencies of C−H stretch vibrations in other molecules as well, for example, in methanol the splitting is 154.8 cm^{-1}.[45]

B. Infrared Spectra of the First Overtone of the OH Stretch ($2\nu_1$). Rotational structure is still present in the spectrum of the first overtone transition of the OH stretch ($2\nu_1$) as shown in Figure 2d, but the linewidth has increased to 0.8 cm^{-1}. This linewidth was independent of IR laser energy in the range 3−5 mJ. The regularity of the rotational structure indicates that IVR is not extensive at this energy region even though the internal energy of the radical ($\sim$7160 cm^{-1}) is almost half of the barrier heights to isomerization ($\sim$14 000 cm^{-1})[8,12] and O−H bond
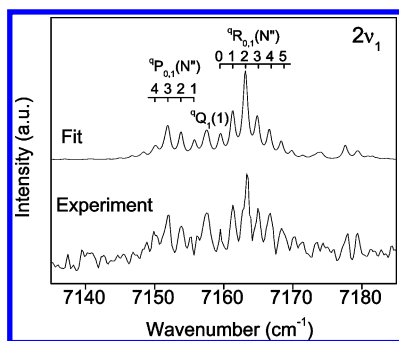
Figure 5. Spectrum of the first overtone of the OH stretch ($2\nu_1$) with assignment. Top: fit; bottom: observed DRID-IR spectrum obtained with 4 mJ IR energy.

TABLE 2: Observed Energies and Linewidths, and Calculated Density of States

band	energy (cm^{-1})	homogeneous linewidth (cm^{-1})	density of states[a] (1/cm^{-1})
$1\nu_1$ OH stretch	3674.8	≤ 0.4	1
$2\nu_1$ OH stretch	7158.0	0.8 ± 0.1	5

[a] Calculated by the Beyer−Swinehart algorithm.[47]

dissociation ($\sim$16 000 cm^{-1}).[7,8] The $2\nu_1$ spectrum is modeled by a similar procedure to that used for the fundamental transitions. The only difference is that a Lorentzian linewidth is varied to obtain a best fit to the data (0.8 ± 0.1 cm^{-1}) instead of fixing it at the IR laser bandwidth (0.4 cm^{-1}). The same linewidth is used for all the rotational levels. In Figure 5, the fit is compared with the corresponding DRID-IR overtone spectrum. The rotational constants of the overtone obtained from the least-squares fit are $A_2 = 6.39 \pm 0.02$ cm^{-1}, $B_2 = 0.97 \pm 0.02$ cm^{-1}, $C_2 = 0.88 \pm 0.01$ cm^{-1}. The results are summarized in Table 2.

Typically, transition frequencies for light atom stretches follow the Birge−Sponer relation. For the OH stretch vibration in CH$_2$OH, the frequencies for the fundamental and first overtone should follow the relation $\Delta\nu/\nu = A + B\nu$, where $\Delta\nu$ is the transition frequency in wavenumber, $\omega_e = A - B$ is the mechanical frequency, and $\omega_e\chi_e = -B$ is the anharmonicity. The OH stretch anharmonicity for CH$_2$OH obtained in this work is 95.9 cm^{-1}. Although this value is limited only to the first overtone and may need to be refined for higher overtone frequencies, it is comparable to the anharmonicity parameters for the OH-stretch mode in methanol and NH$_2$OH, which are 86 and 91 cm^{-1}, respectively.[45,46] The value for CH$_2$OH is slightly higher than these values, apparently reflecting its lower barrier to dissociation.

Referring to the observed increase in rotational linewidth, several issues should be considered. First, because of the large bandwidth (0.4 cm^{-1}) of our IR laser beam, we cannot distinguish between a homogeneous linewidth and the spectral overlap of a few sharp transitions involving mixed states that borrow oscillator strength from the "bright" OH overtone. A calculation of the vibrational density of states ρ, using the Beyer−Swinehart algorithm and neglecting anharmonicity,[47] gives $\rho = \sim$5 states per cm^{-1} in the region of $2\nu_1$ (Table 2). However, restricting the coupling to low-order resonances (i.e., combination levels with a total number of quanta less than six) reduces the density of effectively coupled states to less than one state per cm^{-1}.

In the OH overtone transitions of CH$_3$OH and NH$_2$OH, homogeneous broadening was observed starting from the second overtone OH-stretch ($3\nu_1$).[45,46] CH$_2$OH has a lower barrier to dissociation than these molecules, which may cause enhanced anharmonic coupling to other modes even in the first overtone. Also, CH$_2$OH has a higher density of states than NH$_2$OH and a lower barrier to internal rotation, and therefore its IVR threshold may be reached at lower energies. On the other hand, the NH$_2$OH results were obtained with 300 K samples, where Coriolis couplings may be significant. Also, in methanol the low torsional barrier ($\sim$400 cm^{-1}, compared to 1600 cm^{-1} in CH$_2$OH) is likely to promote coupling.[48,49] Pursuant to the above discussion, it is unlikely that the cause of the observed line broadening is the onset of IVR to a bath of "dark" states. Rather, it is more plausible that accidental low-order resonances with $2\nu_1$ result in small line splittings around each "bright" state that appear as broadened lines at low resolution. Such resonances may include, for example, $1\nu_8 + 1\nu_3 + 1\nu_1$. Individual transitions to molecular eigenstates may be revealed in experiments carried out at higher resolution. With our resolution and S/N, it is hard to tell whether the linewidth is homogeneous and all the rotational transitions have the same linewidth. We expect, however, that the onset of IVR will be reached in the next OH overtone transition, which according to the Birge−Sponer relation should be around 10 449 cm^{-1}, that is, much closer in energy to the dissociation barrier. In this case, IVR may couple each low-order resonance to a bath of dark states, either directly or via a multiple tier system as observed, for example, in methanol.[45]

V. Conclusions

The DRID-IR technique enables investigations of the vibrational spectroscopy of CH$_2$OH in a molecular beam. Rotationally resolved IR spectra are obtained in the region of the fundamental CH symmetric stretch (ν_3), CH asymmetric stretch (ν_2), OH stretch (ν_1), and the OH stretch overtone ($2\nu_1$).

The rovibrational structures of the ν_1, ν_2, and ν_3 bands agree well with fitted spectra derived with the aid of ab intio calculations. The OH- and CH-symmetric stretch vibrational structures are hybrid a/b-type bands, while that of the CH asymmetric stretch fundamental is a pure b-type transition.

Rotational structure is still apparent in the $2\nu_1$ overtone spectrum, indicating that IVR is not extensive in this energy region. An increase in rotational linewidth is observed, which is probably due to spectral overlap of a few transitions around each rotational level of $2\nu_1$ borrowing intensity from the bright OH chromophore. The OH stretch anharmonicity estimated in this work, 95.9 cm^{-1}, is comparable to but slightly higher than the corresponding values in methanol and hydroxylamine. Experimental work is in progress on the spectroscopy of higher vibrational overtones of the OH stretch and on product formation via direct dissociation or isomerization pathways.

References and Notes

(1) Lin, J. J.; Shu, J.; Lee, Y. T.; Yang, X. *J. Chem. Phys.* **2000**, *113*, 5287.

(2) Shu, J.; Lin, J. J.; Lee, Y. T.; Yang, X. M. *J. Chem. Phys.* **2001**, *115*, 849.

(3) Pagsberg, P.; Munk, J.; Sillesen, A.; Anastasi, C.; Simpson, V. *Chem. Phys. Lett.* **1988**, *146*, 375.

(4) Ahmed, M.; Peterka, D. S.; Suits, A. G. *Phys. Chem. Chem. Phys.* **2000**, *2*, 861.

(5) Rudic, S.; Ascenzi, D.; Orr-Ewing, A. J. *Chem. Phys. Lett.* **2000**, *332*, 487.

(6) Rudic, S.; Murray, C.; Ascenzi, D.; Anderson, H.; Harvey, J. N.; Orr-Ewing, A. J. *J. Chem. Phys.* **2002**, *117*, 5692.

(7) Adams, G. F.; Bartlett, R. J.; Purvis, G. D. *Chem. Phys. Lett.* **1982**, *87*, 311.

(8) Saebo, S.; Radom, L.; Schaefer, H. F. *J. Chem. Phys.* **1983**, *78*, 845.

(9) Dertinger, S.; Geers, A.; Kappert, J.; Wiebrecht, J.; Temps, F. *Faraday Discuss.* **1995**, 31.

(10) Dobe, S.; Berces, T.; Turanyi, T.; Marta, F.; Grussdorf, J.; Temps, F.; Wagner, H. G. *J. Phys. Chem.* **1996**, *100*, 19864.

(11) Oehlers, C.; Wagner, H. G.; Ziemer, H.; Temps, F.; Dobe, S. *J. Phys. Chem. A* **2000**, *104*, 10500.

(12) Hippler, H.; Striebel, F.; Viskolcz, B. *Phys. Chem. Chem. Phys.* **2001**, *3*, 2450.

(13) Walch, S. P. *J. Chem. Phys.* **1993**, *98*, 3076.

(14) Johnson, R. D.; Hudgens, J. W. *J. Phys. Chem.* **1996**, *100*, 19874.

(15) Marenich, A. V.; Boggs, J. E. *J. Chem. Phys.* **2003**, *119*, 3098.

(16) Marenich, A. V.; Boggs, J. E. *J. Chem. Phys.* **2003**, *119*, 10105.

(17) Aristov, V.; Conroy, D.; Reisler, H. *Chem. Phys. Lett.* **2000**, *318*, 393.

(18) Dulcey, C. S.; Hudgens, J. W. *J. Phys. Chem.* **1983**, *87*, 2296.

(19) Dulcey, C. S.; Hudgens, J. W. *Bull. Soc. Chim. Belg.* **1983**, *92*, 583.

(20) Dulcey, C. S.; Hudgens, J. W. *J. Chem. Phys.* **1986**, *84*, 5262.

(21) Feng, L.; Huang, X.; Reisler, H. *J. Chem. Phys.* **2002**, *117*, 4820.

(22) Hoffman, B. C.; Yarkony, D. R. *J. Chem. Phys.* **2002**, *116*, 8300.

(23) Feng, L.; Demyanenko, A. V.; Reisler, H. *J. Chem. Phys.* **2004**, *120*, 6524.

(24) Jacox, M. E.; Milligan, D. E. *J. Mol. Spectrosc.* **1973**, *47*, 148.

(25) Jacox, M. E.; *Chem. Phys.* **1981**, *59*, 213.

(26) Page, R. H.; Shen, Y. R.; Lee, Y. T. *J. Chem. Phys.* **1988**, *88*, 5362.

(27) Donovan, R. J.; Ridley, T.; Lawley, K. P.; Wilson, P. *Chem. Phys. Lett.* **1992**, *196*, 173.

(28) Fehrensen, B.; Hippler, M.; Quack, M. *Chem. Phys. Lett.* **1998**, *298*, 320.

(29) Hippler, M.; Pfab, R.; Quack, M. *J. Phys. Chem. A* **2003**, *107*, 10743.

(30) Conroy, D.; Aristov, V.; Feng, L.; Reisler, H. *J. Phys. Chem. A* **2000**, *104*, 10288.

(31) Herzberg, G. *Infrared and Raman Spectra of Polyatomic Molecules*; D. Van Nostrand Company, Inc.: New York, 1945; p 454.

(32) Schaeffer, M. W.; Kim, W.; Maxton, P. M.; Romascan, J.; Felker, P. M. *Chem. Phys. Lett.* **1995**, *242*, 632.

(33) Pribble, R. N.; Hagemeister, F. C.; Zwier, T. S. *J. Chem. Phys.* **1997**, *106*, 2145.

(34) Stearns, J. A.; Zwier, T. S. *J. Phys. Chem. A* **2003**, *107*, 10717.

(35) Feng, L.; Reisler, H. *J. Phys. Chem. A* **2004**, submitted.

(36) Rueda, D.; Boyark, O.; Rizzo, T. *J. Chem. Phys.* **2002**, *116*, 91.

(37) Luckhaus, D. *J. Chem. Phys.* **1997**, *106*, 8409.

(38) Stanton, J. F.; Gauss, J.; Watts, J. D.; Lauderdale, W. J.; Bartlett, R. J. ACS II, 1993. The package also contains modified versions of the MOLECULE Gaussian integral program of Almlof, J. and Taylor, P. R., the ABACUS intergal derivative program written by Helgaker, T. U., Jensen, H. J. Aa., Jorgensen, P. and Taylor, P. R., and the PROPS property evaulation integral code of Taylor, P. R.

(39) Piecuch, P.; Kucharski, S. A.; Bartlett, R. J. *J. Chem. Phys.* **1999**, *110*, 6103.

(40) Dunning, T. H. *J. Chem. Phys.* **1989**, *90*, 1007.

(41) Crawford, T. D.; Kraka, E.; Stanton, J. F.; Cremer, D. *J. Chem. Phys.* **2001**, *114*, 10638.

(42) Bruna, P. J.; Grein, F. *J. Phys. Chem. A* **1998**, *102*, 3141.

(43) Bruna, P. J.; Grein, F. *J. Phys. Chem. A* **2001**, *105*, 8599.

(44) Sears, T. J. *Comput. Phys. Commun.* **1984**, *34*, 123.

(45) Boyarkin, O.; Lubich, L.; Settle, R.; Perry, D.; Rizzo, T. *J. Chem. Phys.* **1997**, *107*, 8409.

(46) Scott, J. L.; Luckhaus, D.; Brown, S. S.; Crim, F. F. *J. Chem. Phys.* **1995**, *102*, 675.

(47) Baer, T.; Hase, W. L. *Unimolecular reaction dynamics;* Oxford: New York, 1996; p 183.

(48) Bethardy, G. A.; Wang, X. L.; Perry, D. S. *Can. J. Chem.* **1994**, *72*, 652.

(49) Perry, D. S.; Bethardy, G. A.; Wang, X. L. *Ber. Bunsen-Ges. Phys. Chem.* **1995**, *99*, 530.